Supplemental Document

Biomedical Optics EXPRESS

Brain virtual histology with X-ray phase-contrast tomography Part I:whole-brain myelin mapping in white-matter injury models: supplement

Matthieu Chourrout,[1,11] Hugo Rositi,[2,11] Elodie Ong,[3,4] Violaine Hubert,[3] Alexandre Paccalet,[3] Louis Foucault,[5] Awen Autret,[6] Barbara Fayard,[6] Cécile Olivier,[7] Radu Bolbos,[8] Françoise Peyrin,[7] Claire Crola-da-Silva,[3] David Meyronet,[4] Olivier Raineteau,[5] Héléne Elleaume,[9] Emmanuel Brun,[9] Fabien Chauveau,[1,10,12] and Marlene Wiart[3,10,12,*]

[1] *Univ-Lyon, Lyon Neuroscience Research Center, CNRS UMR5292, Inserm U1028, Université Claude Bernard Lyon 1, Lyon, France*
[2] *Univ-Clermont Auvergne; CNRS; SIGMA Clermont; Institut Pascal, Clermont-Ferrand, France*
[3] *Univ-Lyon, CarMeN laboratory, Inserm U1060, INRA U1397, Université Claude Bernard Lyon 1, INSA Lyon, Charles Mérieux Medical School, F-69600, Oullins, France*
[4] *Univ-Lyon, Hospices Civils de Lyon, Lyon, France*
[5] *Univ-Lyon, Université Claude Bernard Lyon 1, Inserm, Stem Cell and Brain Research Institute U1208, 69500 Bron, France*
[6] *NOVITOM, Grenoble, France*
[7] *Univ-Lyon, INSA-Lyon, Université Claude Bernard Lyon 1, CNRS, Inserm, CREATIS UMR5220, U1206, F-69621, France*
[8] *Cermep, Lyon, France*
[9] *Université Grenoble Alpes, Inserm UA7 Strobe, Grenoble, France*
[10] *CNRS, Lyon, France*
[11] *Co-first authors*
[12] *Co-last authors*
[*] *marlene.wiart@univ-lyon1.fr*

This supplement published with Optica Publishing Group on 23 February 2022 by The Authors under the terms of the Creative Commons Attribution 4.0 License in the format provided by the authors and unedited. Further distribution of this work must maintain attribution to the author(s) and the published article's title, journal citation, and DOI.

Supplement DOI: https://doi.org/10.6084/m9.figshare.16941094

Parent Article DOI: https://doi.org/10.1364/BOE.438832

Brain virtual histology with X-ray phase-contrast tomography — Part I: whole-brain myelin mapping in white-matter injury models — Supplemental document

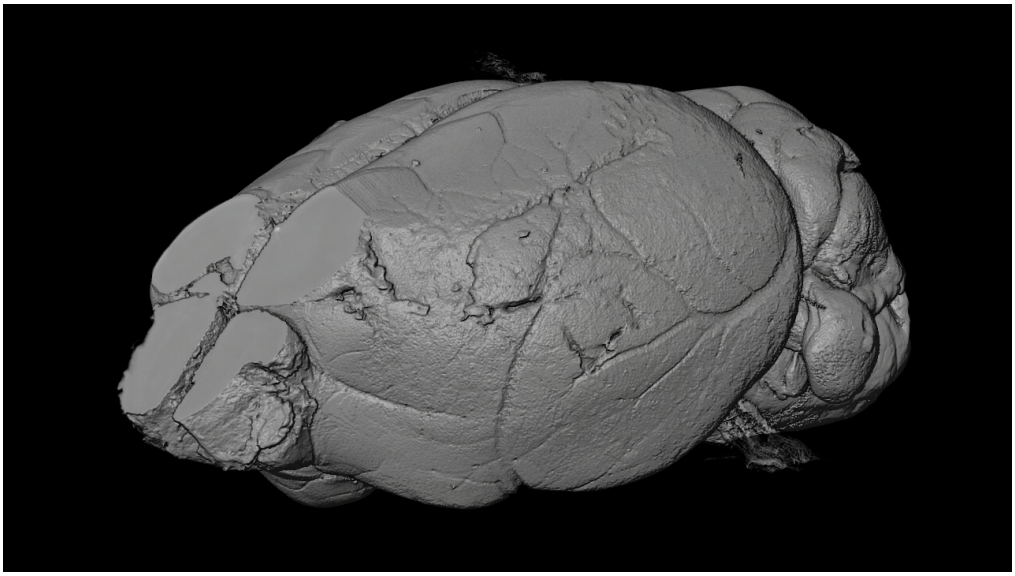

Visualization 1. 3D rendering of a whole mouse brain and virtual histology in coronal view.
URL: https://osapublishing.figshare.com/s/8b5ff8dc95b502237a09

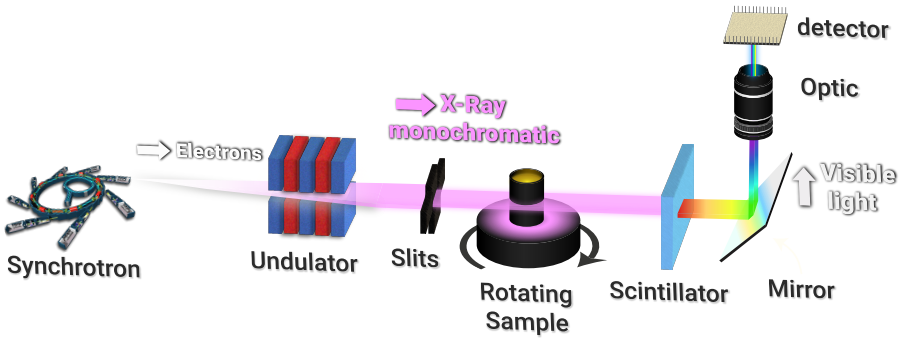

Fig. S1. Principle of in-line phase contrast tomography: experimental set-up

Table S1. Experimental MRI parameters. TE: echo time; TR: repetition time; T2WI: T2-weighted MRI; DTI: diffusion tensor imaging; N/A: non-applicable.

MR imaging parameterkjkkljs	**T2WI**	**DTI**
Spatial acquisition dimension	2D	3D
Measuring method	SpinEcho	DtiEpi
TE [ms]	69.1	25.1
TR [ms]	4000	650
Number of diffusion directions	N/A	30
Number of A0 images	N/A	5
Max. B value [s/mm^2]	N/A	1600
Number of segments	N/A	2
Number of averages	2	1
Bandwidth [kHz]	25	300
Field of view [mm^2 | mm^3]	20×20	$20 \times 10 \times 17$
Slice thickness or interslice [mm]	1	0.5
Number of slices	10	36
Matrix size [pixels]	256×256	$192 \times 96 \times 36$
In-plane resolution [µm^2]	78×78	104×104
Acquisition time [s]	192	1638

Table S2. Experimental XPCT parameters

Figures	1, 2, 4C-D, 5, 6A-B, 7B	3C-D, 4E-F, 6D-E, 6G-H	3A-B
Supplemental Figures	4, 5E-F	5C-D	5A
Setup	ID19	ID19	ID17
Detector	FReLoN	sCMOS (PCO edge)	sCMOS (PCO edge)
Scintillator	LuAg (500 µm)	LuAg (500 µm)	LuAg (500 µm)
Energy [keV] **(**ΔE [eV]**)**	19 (600)	26 (600)	35 (35)
Sample-detector distance [m]	1	1.3–3	11
Field-of-view [cm^3]	$1.5 \times 1.5 \times 1.5$	$1.3 \times 1.3 \times 1.23$	$1.5 \times 1.5 \times 1.5$
Matrix	2048×2048	2048×2048	2560×2160
Total number of slices	2000	2000	3200
Voxel size (isotropic) [µm]	7.5	6.5	6.13
Exposure time [s]	0.15	0.05	0.05
Number of projections	2000 (180°)	2499 (180°)	2800 (360°)
Estimated dose [Gy]	150 000	35 000	60
Acquisition time [min]	< 10		
Reconstruction algorithm	PyHST 2 (Paganin filter, $\delta/\beta \in [600; 1000]$)		

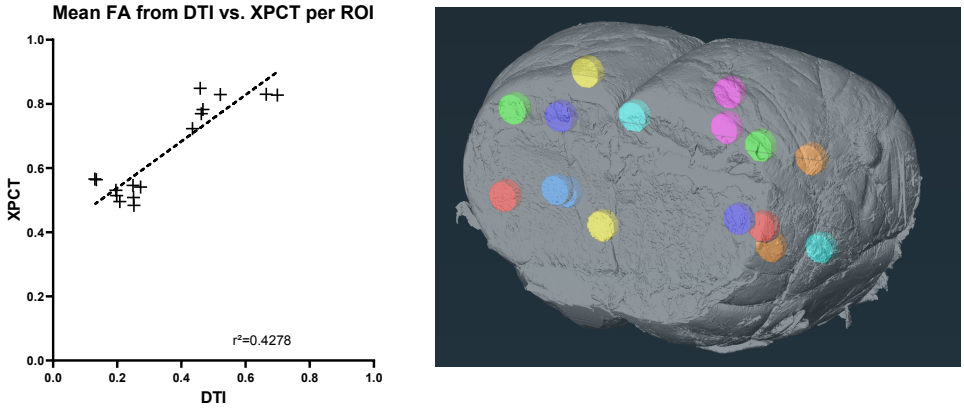

Fig. S2. Comparison of mean FA between in vivo DTI and ex vivo XPCT

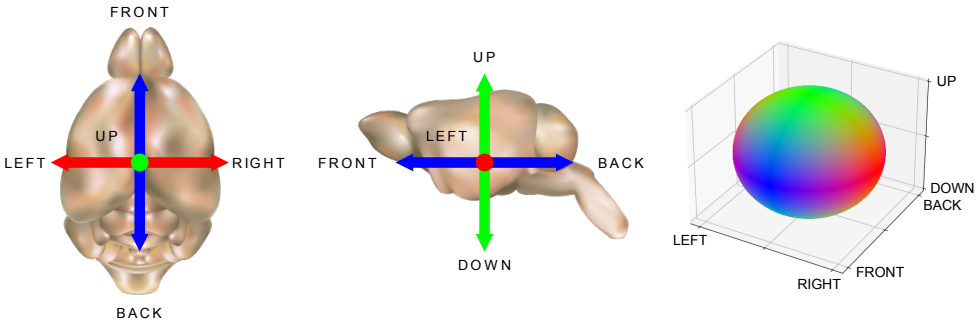

Fig. S3. Color-code convention for fiber orientation from the diffusion MRI community. It is replicated in the NOVITOM software.

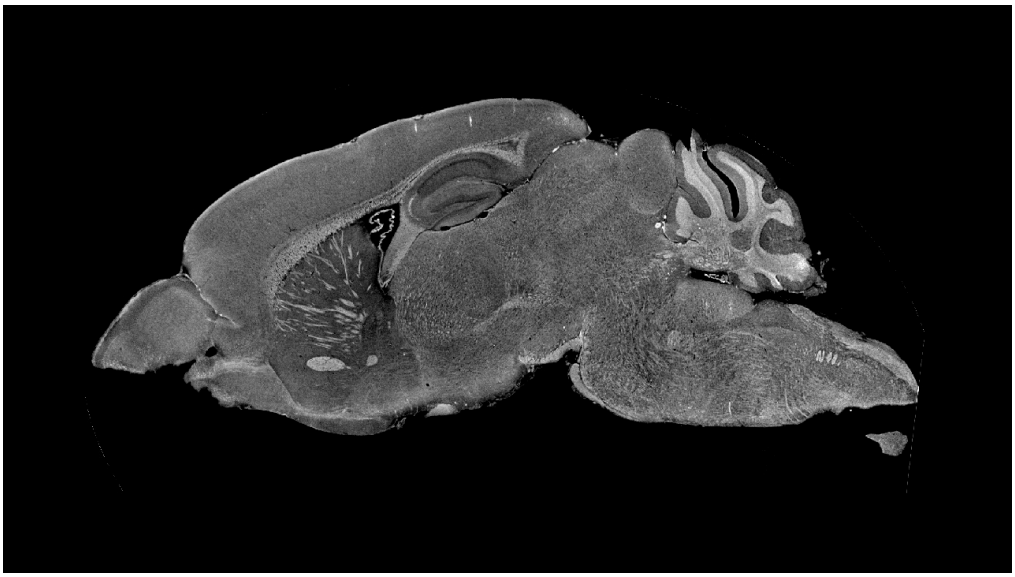

Visualization 2. Virtual histology of a whole mouse brain in sagittal view. URL: https://osapublishing.figshare.com/s/b3288191f556cfd27b99

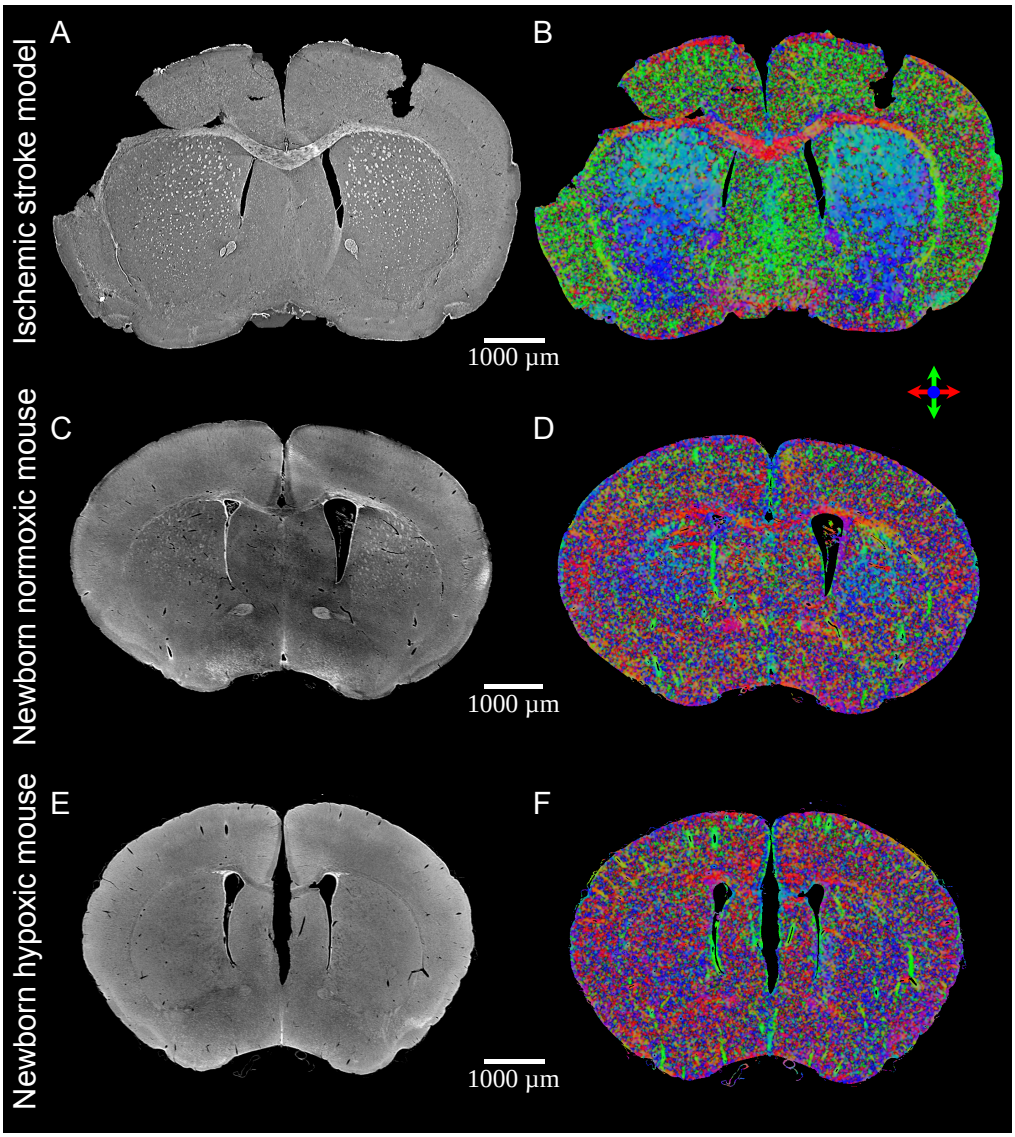

Fig. S4. XPCT retrieves brain-wide structural connectivity in a DTI-like manner. **(A)** Native (single coronal slice) XPCT image of mouse #1 (ischemic stroke model, from Table 2); **(B)** Color-coded direction maps extracted from the same dataset (cf. Fig. S3); **(C)** Native (single coronal slice) XPCT image of mouse #4 (normoxic mouse); **(D)** Color-coded direction maps extracted from the same dataset; **(E)** Native (single coronal slice) XPCT image of mouse #6 (hypoxic mouse); **(F)** Color-coded direction maps extracted from the same dataset. As expected, the newborn normoxic brain is not completely myelinated yet but some of the major fiber tracts are visible (corpus callosum and anterior commissure), whereas they are not observed in the newborn mouse that underwent hypoxia.

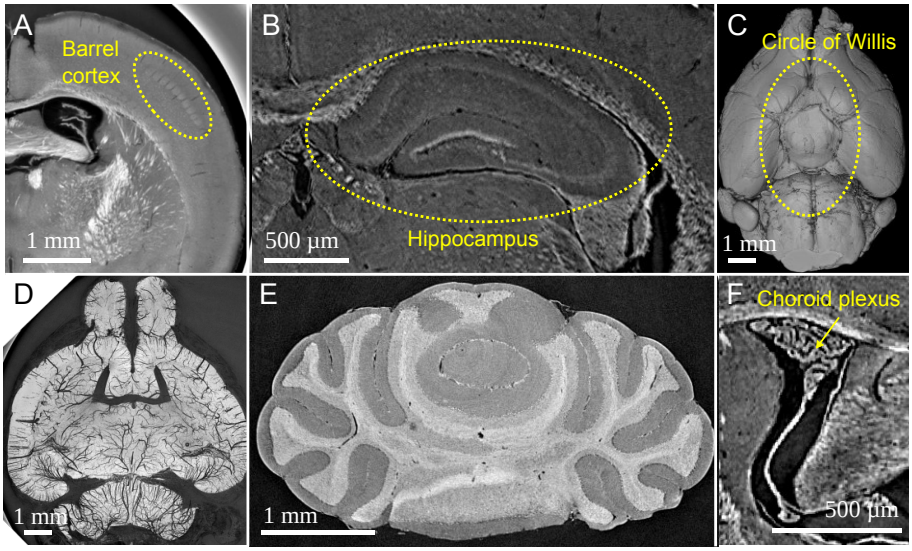

Fig. S5. Virtual histology with XPCT displays major brain anatomic features in the whole mouse brain taken from different samples. (A) Barrel cortex; (B) Hippocampus; (C) Circle of Willis obtained by surface rendering of the whole brain (rostral side); (D) Angiography obtained by minimum intensity projection over 100 slices; (E) Cerebellum; (F) Choroid plexus.